



This is the peer reviewed version of the following article: Mármol-Sánchez, E., R. Quintanilla, J. Jordana, and M. Amills. 2019. "An Association Analysis For 14 Candidate Genes Mapping To Meat Quality Quantitative Trait Loci In A Duroc Pig Population Reveals That The ATP 1A2 Genotype Is Highly Associated With Muscle Electric Conductivity". *Animal Genetics* 51 (1): 95-100. doi:10.1111/age.12864., which has been published in final form at <https://doi.org/10.1111/age.12864>. This article may be used for non-commercial purposes in accordance with Wiley Terms and Conditions for Use of Self-Archived Versions <http://www.wileyauthors.com/self-archiving>.

Document downloaded from:



1 **RUNNING HEAD:** Candidate gene analysis for pig meat quality

2

3 **An association analysis for 14 candidate genes mapping to meat quality QTL in a**
4 **Duroc pig population reveals that the *ATPIA2* genotype is highly associated with**
5 **muscle electric conductivity**

6

7 Emilio Mármol-Sánchez¹, Raquel Quintanilla², Jordi Jordana³, Marcel Amills^{1,3}

8

9 ¹Department of Animal Genetics, Centre for Research in Agricultural Genomics (CRAG),
10 CSIC-IRTA-UAB-UB, Campus de la Universitat Autònoma de Barcelona, Bellaterra,
11 Spain.

12 ²Animal Breeding and Genetics Programme, Institute for Research and Technology in Food
13 and Agriculture (IRTA), Torre Marimon, Caldes de Montbui, Spain.

14 ³Departament de Ciència Animal i dels Aliments, Universitat Autònoma de Barcelona,
15 Bellaterra, Spain.

16

17 Address for correspondence: Marcel Amills, Department of Animal Genetics, Centre for
18 Research in Agricultural Genomics (CRAG), CSIC-IRTA-UAB-UB, Campus de la
19 Universitat Autònoma de Barcelona, Bellaterra 08193, Spain. E-mail:

20 marcel.amills@uab.cat. Tel. +34 93 563 6600

21

22

23

24

25 **Summary**

26

27 In previous genome-wide association studies carried out in a Duroc commercial line
28 (Lipgen population), we detected on pig chromosomes 3, 4 and 14 several QTL for *gluteus*
29 *medius* muscle redness (GM a*), electric conductivity in the *longissimus dorsi* muscle (LD
30 CE) and vaccenic acid content in the LD muscle (LD C18:1 n-7), respectively. We have
31 genotyped, in the Lipgen population, 19 single nucleotide polymorphisms (SNP) mapping to
32 14 genes located within these three QTL. Subsequently, association analyses have been
33 performed. After correction for multiple testing, two SNPs in the *TGFBRAP1* (rs321173745)
34 and *SELENOI* (rs330820437) genes were associated with GM a*, while *ACADSB*
35 (rs81449951) and *GPR26* (rs343087568) genotypes displayed significant associations with
36 LD vaccenic content. Moreover, the polymorphism of the *ATPIA2* (rs344748241), *ATP8B2*
37 (rs81382410) and *CREB3L4* (rs321278469 and rs330133789) genes showed significant
38 associations with LD CE. We made a second round of association analyses including the
39 SNPs mentioned above as well as other SNPs located in the chromosomes to which they map
40 to. After performing a correction for multiple testing, the only association that remained
41 significant at the chromosome-wide level was that between the *ATPIA2* genotype and LD
42 CE. From a functional point of view, this association is meaningful because this locus
43 encodes a subunit of the Na⁺/K⁺-ATPase responsible of maintaining an electrochemical
44 gradient across the plasma membrane.

45

46 **Keywords:** Pig, single nucleotide polymorphism, meat quality, Na⁺/K⁺-ATPase.

47

48

49 Meat quality traits are of paramount importance for the pig industry because they
50 determine, to a great extent, consumer acceptance and financial profit. Once pigs are
51 slaughtered, there is a decline of the pH of the skeletal muscle due to the production of lactic
52 acid through anaerobic glycolysis (Rosenvold & Andersen 2003). The rate of muscle
53 acidification has a strong effect on meat color and water-holding capacity. In this way, a low
54 ultimate pH (5.4-5.3) is associated with pale, soft and exudative (PSE) meat as well as with
55 an increased electrical conductivity (CE) and elevated drip and cooking losses (Lee *et al.*
56 2000; Rosenvold & Andersen 2003). In contrast, a high ultimate pH (6.3 or higher) results in
57 dark, firm and dry (DFD) meat with a high water-holding capacity and a lower CE (Lee *et*
58 *al.* 2000; Kim *et al.* 2016). Adverse effects on meat quality are influenced by both genetic
59 and environmental factors. Recessive and dominant genotypes in the porcine ryanodine
60 receptor 1 (*RYR1*) and the protein kinase AMP-activated non-catalytic subunit γ_3 (*PRKAG3*)
61 genes, respectively, are strong predisposing factors to the occurrence of PSE meats (Fujii *et*
62 *al.* 1991; Milan *et al.* 2000). On the other hand, there are multiple factors related with pig
63 management and transportation (pre-slaughter stress), stunning method at slaughter, carcass
64 chilling and pelvic suspension of carcasses that influence pork quality (Rosenvold &
65 Andersen 2003). Another important parameter that determines meat quality is intramuscular
66 fat (IMF) composition. In this regard, it is well known that fatty acid composition can have
67 important consequences on the oxidative stability of meat during processing and retail
68 display as well as on fat firmness (Wood *et al.* 2008).

69 In previous genome-wide association studies, we identified several genomic regions
70 containing quantitative trait loci (QTL) for meat Minolta a^* value (redness), CE (González-
71 Prendes *et al.* 2017) and IMF composition (González-Prendes *et al.* 2019) traits measured in
72 the *longissimus dorsi* (LD) and *gluteus medius* (GM) muscle samples of 350 Duroc barrows

73 (Lipgen population). Details about the rearing of the Lipgen pigs can be found in Gallardo *et*
74 *al.* (2009), while a thorough description of QTL mapping methods is reported in González-
75 Prendes *et al.* (2017). The measurement of CE was done 24 hours after slaughter by using a
76 Pork Quality Meter (Intek GmbH), while Minolta a* value was determined with a Minolta
77 Chroma-Meter CR-200 (Konica Minolta) equipment at the same time point. Muscle fatty
78 acid composition was measured as previously described by Quintanilla *et al.* (2011). In the
79 current work, we have selected 14 candidate genes located within QTL regions for GM a*
80 on SSC3, LD CE on SSC4, and LD vaccenic content on SSC14 (**Table 1**). These genes were:
81 phosphorylase kinase catalytic subunit γ 1 (*PHKGI*), transforming growth factor β receptor
82 associated protein 1 (*TGFBRAP1*), selenoprotein I (*SELENOI*), hydroxyacyl-CoA
83 dehydrogenase trifunctional multienzyme (*HADHA*), coatomer protein complex subunit α
84 (*COPA*), proliferation and apoptosis adaptor protein 15 (*PEA15*), calsequestrin 1 (*CASQ1*),
85 ATPase Na⁺/K⁺ transporting α_2 subunit (*ATPIA2*), ATPase phospholipid transporting 8B2
86 (*ATP8B2*), cAMP responsive element binding protein 3 like 4 (*CREB3L4*), CREB regulated
87 transcription coactivator 2 (*CRTC2*), acyl-CoA dehydrogenase short/branched chain
88 (*ACADSB*), G protein-coupled receptor 26 (*GPR26*) and C-terminal binding protein 2
89 (*CTBP2*).

90 Genes were selected based on bibliographic information about their biological
91 functions which suggested that they could be involved in the determinism of meat quality.
92 Based on available RNA-Seq (Cardoso *et al.* 2017) and whole-genome data (our unpublished
93 results), we called 19 SNPs mapping to these 14 genes by using the GATK Best Practices
94 workflow for SNP calling ([https://software.broadinstitute.org/gatk/best-](https://software.broadinstitute.org/gatk/best-practices/workflow?id=11145)
95 [practices/workflow?id=11145](https://software.broadinstitute.org/gatk/best-practices/workflow?id=11145)) in accordance with protocols reported by Mármol-Sánchez *et*
96 *al.* (2019). Nineteen SNPs were finally selected because the SnpEff software predicted that

97 they might have functional effects (Cingolani *et al.* 2012), as reported in **Supplementary**
98 **Table 1**. The 19 selected SNPs (**Table 1**) were genotyped at the Servei Veterinari de Genètica
99 Molecular of the Universitat Autònoma de Barcelona (<http://set.uab.cat/svgn/en>) by using a
100 QuantStudio 12K Flex Real-Time PCR System (ThermoFisher Scientific). Association
101 analyses between SNPs and phenotypes were performed with the Genome-wide Efficient
102 Mixed-Model Association (GEMMA) software (Zhou & Stephens 2012). The following
103 statistical model was used:

104

$$105 \mathbf{y} = \mathbf{W}\boldsymbol{\alpha} + \mathbf{x}\boldsymbol{\delta} + \mathbf{u} + \boldsymbol{\varepsilon}$$

106

107 where \mathbf{y} is the vector of phenotypic observations for every individual; $\boldsymbol{\alpha}$ corresponds
108 to a vector including the intercept plus the fixed effects, *i.e.* batch effect with 4 categories
109 (all traits), and farm origin effect with 3 categories (all traits). The $\boldsymbol{\alpha}$ vector also contains the
110 regression coefficients of the following covariates: (1) Carcass weight at slaughterhouse for
111 meat quality traits, and (2) IMF content in the LD muscle for LD fatty acid composition; \mathbf{W}
112 is the incidence matrix relating phenotypes with the corresponding effects; \mathbf{x} is the vector of
113 the genotypes corresponding to the set of selected polymorphisms; $\boldsymbol{\delta}$ is the allele substitution
114 effect for each polymorphism; \mathbf{u} is a vector of random individual effects with a n-dimensional
115 multivariate normal distribution $MVN_n(0, \lambda \tau^{-1} \mathbf{K})$, where τ^{-1} is the variance of the residual
116 errors, λ is the ratio between the two variance components and \mathbf{K} is a known relatedness
117 matrix derived from the SNPs; and $\boldsymbol{\varepsilon}$ is the vector of residual errors. Results were corrected
118 for multiple testing by using the false discovery rate (FDR) method reported by Benjamini
119 & Hochberg (1995). The correction for multiple testing took into account the number of

120 candidate SNPs (2nd column of **Table 1**) mapping to each one of the SSC3 GM a* (5 SNPs),
121 SSC4 LD CE (11 SNPs) and SSC14 LD (C18:1) n-7 (3 SNPs) QTL.

122 Performance of association analyses with the methodology described above revealed
123 the existence of several associations that remained significant even after correction for
124 multiple testing. We have found, for instance, an association between GM Minolta a* value
125 and missense mutations in the *TGFBRAP1* and *SELENOI* genes, which map to two different
126 GM a* QTL on SSC3 (**Table 1**). The inactivation of the *TGFBRAP1* gene results in the
127 suppression of aerobic glycolysis and increased levels of mitochondrial respiration and fatty
128 acid oxidation (Yoshida *et al.* 2013), while *SELENOI* encodes a selenoprotein fundamental
129 for the synthesis of phosphatidylethanolamine, a molecule with important effects on the
130 oxidation of lipid membranes, oxidative phosphorylation and mitochondrial morphology
131 (Tasseva *et al.* 2013; Poyton *et al.* 2016). We have also detected significant associations
132 between LD CE and SNPs in the *ATPIA2*, *ATP8B2* and *CREB3L4* genes, which map to SSC4
133 LD CE QTL covering two regions spanning from 85.6 to 91 Mb and from 95.2 to 97.8 Mb.
134 These findings are very suggestive because the *ATPIA2* gene, the one showing the most
135 significant association, is preferentially expressed in the skeletal and heart muscle and brain
136 and it encodes the α_2 subunit of the ion pump Na^+/K^+ ATPase (Clausen *et al.* 2017).
137 Noteworthy, Na^+/K^+ -ATPases provide the energy necessary for the maintenance of Na^+ and
138 K^+ electrochemical gradients across the plasma membrane by hydrolyzing ATP (Clausen *et*
139 *al.* 2017; Sampedro *et al.* 2018). These gradients are essential for the preservation of the
140 resting membrane potential as well as for the generation of electrical impulses in the skeletal
141 muscle and nervous system (Clausen *et al.* 2017; Sampedro *et al.* 2018). The ATP8B2 protein
142 is also an ATPase with flippase activity towards phosphatidyl choline, a key component of

143 phospholipid membranes with important effects on the functioning of the sarcoendoplasmic
144 reticulum Ca^{2+} ATPase pumps (Shin & Takatsu 2018; Fajardo *et al.* 2018), while CREB3L4
145 is a transmembrane bZip transcription factor involved in the modulation of endoplasmic
146 reticulum stress (Kim *et al.* 2014). Our association analysis has also revealed the existence
147 of significant associations between the phenotypic variation of LD vaccenic (C18:1 n-7)
148 content and SSC14 SNPs located in the *ACADSB* gene, which catalyzes the oxidation of
149 branched-chain fatty acids (Porta *et al.* 2019) and the *GPR26* gene, whose inactivation leads
150 to hyperphagia, glucose intolerance, hyperinsulinemia, dyslipidemia and obesity in mice
151 (Chen *et al.* 2012).

152 We have made a second round of association analyses in which the SNPs that
153 previously showed evidence of statistical significance were compared against the whole sets
154 of the Porcine SNP60 BeadChip SNPs co-localizing to the same chromosome (chromosome-
155 wide analysis) *i.e.* 3,123 SNPs on SSC3, 3,899 SNPs on SSC4 and 4,203 SNPs on SSC14.
156 These 11,225 SNPs were obtained from previously published porcine SNP60 BeadChip data
157 reported by González-Prendes *et al.* (2017). In this case, the correction for multiple testing
158 took into account the number of SNPs mentioned above for each one of the three
159 chromosomes under analysis, *i.e.* 3,128, 3,910 and 4,206 independent tests were taken into
160 consideration when performing association analyses for pig chromosomes SSC3, SSC4 and
161 SSC14. Interestingly, the rs344748241 SNP in the *ATPIA2* gene was the only one that
162 surpassed the chromosome-wide threshold of significance (q-value < 0.05) (**Table 1, Figure**
163 **1**). Noteworthy, this SNP was not significant when we made an association analysis at the
164 genome-wide level (data not shown). Additionally, we used the *LD* function of the *gaston* R
165 package (v1.5.5; Perdry & Dandine-Roulland 2019) to evaluate the presence of linkage
166 disequilibrium among the SNP markers that showed significant associations with LD CE

167 after correction for multiple testing at the chromosome-wide level (**Supplementary Figure**
168 **1**). The amount of linkage disequilibrium was expressed as r^2 in accordance with the
169 definition of Hill & Robertson (1968). As shown in **Supplementary Figure 1**, we observed
170 a high degree of linkage disequilibrium between the rs344748241 (*ATPIA2* gene) and the
171 rs80782100 (*IGSF8* gene) markers. Noteworthy, the rs80782100 SNP, which maps to an
172 intronic position within the immunoglobulin superfamily member 8 gene, displays the
173 highest association with the LD CE phenotype, as described in González-Prendes *et al.*
174 (2017).

175 As previously discussed, we consider that the *ATPIA2* gene is a strong positional and
176 functional candidate to explain the CE QTL found on SSC4 because Na^+ , K^+ ATPases are
177 fundamental to induce an electrochemical gradient across the plasma membrane of cells
178 (Suhail 2010), and their kinetics are modulated by the extracellular pH (Salonikidis *et al.*
179 2000), a parameter which also displays strong effects on muscle electrical conductivity. In
180 pigs, the *ATPIA2* gene has been sequenced (Henriksen *et al.* 2013) and its polymorphisms
181 have been associated with fat cut percentage (Fontanesi *et al.* 2012). A next step would be to
182 re-sequence the whole gene in Lipgen pigs with alternative genotypes (QQ vs qq) for the LD
183 CE QTL on SSC4, to build a complete catalogue of SNPs with potential effects on protein
184 activity and expression and to investigate their association with CE in the Lipgen population.
185 Subsequently, functional tests should be applied to ascertain whether any of the mutations in
186 the pig *ATPIA2* gene with highly significant q -values also have causal effects on muscle
187 conductivity.

188

189 **Acknowledgments**

190

191 The authors are indebted to Selecció Batallé S.A. for providing the animal material
192 used in this study. We gratefully acknowledge J. Reixach and J. Soler (IRTA) for their
193 collaboration in the experimental protocols. This research was partially funded with grants
194 AGL2013-48742-C2-1-R and AGL2013-48742-C2-2-R awarded by the Spanish Ministry of
195 Economy and Competitiveness and grant 2014 SGR 1528 from the Agency for Management
196 of University and Research Grants of the Generalitat de Catalunya. Emilio Mármol-Sánchez
197 was funded with a FPU Ph.D. grant from the Spanish Ministry of Education (FPU15/01733).
198 We also acknowledge the support of the Spanish Ministry of Economy and Competitiveness
199 for the Center of Excellence Severo Ochoa 2016-2019 (SEV-2015-0533) grant awarded to
200 the Center for Research in Agricultural Genomics. Thanks also to the CERCA Programme
201 of the Generalitat de Catalunya.

202

203 **Data availability**

204

205 These 11,225 SNPs included in this study were obtained from published Porcine SNP60
206 BeadChip data reported by González-Prendes *et al.* (2017), which can be accessed at the
207 Figshare public repository (<https://figshare.com/s/2e636697009360986794>).

208

209 **Conflict of interest**

210

211 The authors declare that they have no conflict of interest.

212

213

214

215 **References**

216

217 Benjamini Y. & Hochberg Y. (1995) Controlling the false discovery rate: a practical and
218 powerful approach to multiple testing. *Journal of the Royal Statistical Society*
219 *Series B (Methodological)* **57**, 289-300.

220 Cardoso T.F., Cánovas A., Canela-Xandri O., González-Prendes R., Amills M. &
221 Quintanilla R. (2017) RNA-seq based detection of differentially expressed genes in
222 the skeletal muscle of Duroc pigs with distinct lipid profiles. *Scientific Reports* **7**,
223 40005.

224 Chen D., Liu X., Zhang W. & Shi Y. (2012) Targeted inactivation of GPR26 leads to
225 hyperphagia and adiposity by activating AMPK in the hypothalamus. *PLoS One* **7**,
226 e40764.

227 Cingolani P., Platts A., Wang Ie L., Coon M., Nguyen T., Wang L., Land S.J., Lu X. &
228 Ruden D.M. (2012) A program for annotating and predicting the effects of single
229 nucleotide polymorphisms, SnpEff: SNPs in the genome of *Drosophila*
230 *melanogaster* strain w1118; iso-2; iso-3. *Fly* **6**, 80-92.

231 Clausen M.V., Hilbers F. & Poulsen H. (2017) The structure and function of the Na,K-
232 ATPase isoforms in health and disease. *Frontiers in Physiology* **8**, 371.

233 Fajardo V.A., Mikhaeil J.S., Leveille C.F., Tupling A.R. & LeBlanc P.J. (2018) Elevated
234 whole muscle phosphatidylcholine: phosphatidylethanolamine ratio coincides with
235 reduced SERCA activity in murine overloaded plantaris muscles. *Lipids in Health*
236 *and Disease* **17**, 47.

237 Fontanesi L., Galimberti G., Calò D.G., Fronza R., Martelli P.L., Scotti E., Colombo M.,
238 Schiavo G., Casadio R., Buttazzoni L. & Russo V. (2012) Identification and

239 association analysis of several hundred single nucleotide polymorphisms within
240 candidate genes for back fat thickness in Italian Large White pigs using a selective
241 genotyping approach. *Journal of Animal Science* **90**, 2450-64.

242 Fujii J., Otsu K., Zorzato F., de Leon S., Khana V.K., Weiler J.E., O' Brien P.J. & McLennan
243 D.H. (1991) Identification of a mutation in porcine ryanodine receptor associated
244 with malignant hyperthermia. *Science* **253**, 448-451.

245 Gallardo D., Quintanilla R., Varona L., Díaz I., Ramírez O., Pena R.N., & Amills M. (2009)
246 Polymorphism of the pig *acetyl-coenzyme A carboxylase α* gene is associated with
247 fatty acid composition in a Duroc commercial line. *Animal Genetics* **40**, 410-419.

248 González-Prendes R., Quintanilla R., Cánovas A., Manunza A., Figueiredo Cardoso T.,
249 Jordana J., Noguera J.L., Pena R.N. & Amills M. (2017) Joint QTL mapping and
250 gene expression analysis identify positional candidate genes influencing pork
251 quality traits. *Scientific Reports* **7**, 39830.

252 González-Prendes R., Quintanilla R., Mármol-Sánchez E., Pena R.N., Ballester M.,
253 Cardoso T.F., Manunza A., Casellas J., Cánovas A., Diaz I., Noguera J.L., Castelló
254 A., Mercade A. & Amills M. (2019) Comparing the mRNA expression profile and
255 the genetic determinism of intramuscular fat traits in the porcine *gluteus medius* and
256 *longissimus dorsi* muscles. *BMC Genomics* **20**, 170.

257 Henriksen C., Kjaer-Sorensen K., Einholm A.P., Madsen L.B., Momeni J., Bendixen C.,
258 Oxvig C., Vilsen B. & Larsen K. (2013) Molecular cloning and characterization of
259 porcine Na⁺/K⁺-ATPase isoforms α_1 , α_2 , α_3 and the ATP1A3 promoter. *PLoS One* **8**,
260 e79127.

261

262 Hill W.G. & Robertson A. (1968) Linkage disequilibrium in finite populations. *Theoretical*
263 *and Applied Genetics* **38**, 226-31.

264 Kim T.H., Jo S.H., Choi H., Park J.M., Kim M.Y., Nojima H., Kim J.W. & Ahn Y.H.
265 (2014) Identification of *Creb3l4* as an essential negative regulator of adipogenesis.
266 *Cell Death & Disease* **5**, e1527.

267 Kim T.W., Kim C.W., Yang M.R., No G.R., Kim S.W. & Kim I.S. (2016) Pork quality
268 traits according to postmortem pH and temperature in Berkshire. *Korean Journal*
269 *for Food Science of Animal Resources* **36**, 29-36.

270 Lee S., Norman J.M., Gunasekaran S., van Laack R.L., Kim B.C. & Kauffman R.G. (2000)
271 Use of electrical conductivity to predict water-holding capacity in post-rigor pork.
272 *Meat Science* **55**, 385-9.

273 Mármol-Sánchez E., Quintanilla R., Cardoso T.F., Jordana J. & Amills M. (2019)
274 Polymorphisms of the cryptochrome 2 and mitoguardin 2 genes are associated with
275 the variation of lipid-related traits in Duroc pigs. *Scientific Reports*. In press. doi:
276 10.1038/s41598-019-45108-z.

277 Milan D., Jeon J.T., Looft C., Amarger V., Robic A., Thelander M., Rogel-Gaillard C., Paul
278 S., Iannuccelli N., Rask L., Ronne H., Lundström K., Reinsch N., Gellin J., Kalm E.,
279 Le Roy P., Chardon P. & Andersson L. (2000) A mutation in *PRKAG3* associated
280 with excess glycogen content in pig skeletal muscle. *Science* **288**, 1248-1251.

281 Perdry H. & Dandine-Roullard C. (2019) gaston: Genetic Data Handling (QC, GRM, LD,
282 PCA) & Linear Mixed Models. R package version 1.5.5. [https://CRAN.R-](https://CRAN.R-project.org/package=gaston)
283 [project.org/package=gaston](https://CRAN.R-project.org/package=gaston)

284 Porta F., Chiesa N., Martinelli D. & Spada M. (2019) Clinical, biochemical and molecular
285 spectrum of short/branched-chain acyl-CoA dehydrogenase deficiency: two new

286 cases and review of literature. *Journal of Pediatric Endocrinology and Metabolism*
287 **32**, 101-108.

288 Poyton M.F., Sendeki A.M., Cong X. & Cremer P.S. (2016) Cu²⁺ binds to
289 phosphatidylethanolamine and increases oxidation in lipid membranes. *Journal of*
290 *the American Chemical Society* **138**, 1584-90.

291 Quintanilla R., Pena R.N., Gallardo D., Cánovas A., Ramírez O., Díaz I., Noguera J.L. &
292 Amills M. (2011) Porcine intramuscular fat content and composition are regulated
293 by quantitative trait loci with muscle-specific effects. *Journal of Animal Science* **89**,
294 2963-71.

295 Rosenvold K. & Andersen H.J. (2003) Factors of significance for pork quality-a review.
296 *Meat Science* **64**, 219-37.

297 Salonikidis P.S., Kirichenko S.N., Tatjanenko L.V., Schwarz W. & Vasilets L.A. (2000)
298 Extracellular pH modulates kinetics of the Na⁺,K⁺-ATPase. *Biochimica et*
299 *Biophysica Acta (BBA) - Biomembranes* **1509**, 496-504.

300 Sampedro Castañeda M., Zanoteli E., Scalco R.S., Scaramuzzi V., Marques Caldas V.,
301 Conti Reed U., da Silva A.M.S., O'Callaghan B., Phadke R., Bugiardini E., Sud R.,
302 McCall S., Hanna M.G., Poulsen H., Männikkö R. & Matthews E. (2018) A novel
303 ATP1A2 mutation in a patient with hypokalaemic periodic paralysis and CNS
304 symptoms. *Brain* **141**, 3308-3318.

305 Shin H.W. & Takatsu H. (2018) Substrates of P4-ATPases: beyond aminophospholipids
306 (phosphatidylserine and phosphatidylethanolamine). *The FASEB Journal* **3**, 3087-
307 3096.

308 Suhail M. (2010) Na, K-ATPase: Ubiquitous multifunctional transmembrane protein and its
309 relevance to various pathophysiological conditions. *Journal of Clinical Medicine*
310 *Research* **2**, 1-17.

311 Tasseva G., Bai H.D., Davidescu M., Haromy A., Michelakis E. & Vance J.E. (2013)
312 Phosphatidylethanolamine deficiency in mammalian mitochondria impairs oxidative
313 phosphorylation and alters mitochondrial morphology. *Journal of Biological*
314 *Chemistry* **288**, 4158-4173.

315 Wood J.D., Enser M., Fisher A.V., Nute G.R., Sheard P.R., Richardson R.I., Hughes S.I. &
316 Whittington F.M. (2008) Fat deposition, fatty acid composition and meat quality: A
317 review. *Meat Science* **78**, 343-58.

318 Yoshida S., Tsutsumi S., Muhlebach G., Sourbier C., Lee M.J., Lee S., Vartholomaiou E.,
319 Tatokoro M., Beebe K., Miyajima N., Mohny R.P., Chen Y., Hasumi H., Xu W.,
320 Fukushima H., Nakamura K., Koga F., Kihara K., Trepel J., Picard D. & Neckers L.
321 (2013) Molecular chaperone TRAP1 regulates a metabolic switch between
322 mitochondrial respiration and aerobic glycolysis. *Proceedings of the National*
323 *Academy of Sciences of the United States of America* **110**, E1604-12.

324 Zhou X. & Stephens M. (2012) Genome-wide efficient mixed-model analysis for
325 association studies. *Nature Genetics* **44**, 821-824.

326 **Table 1.** An association analysis between 19 SNPs mapping to 14 candidate genes and meat quality traits recorded in a Duroc pig
 327 population (significant associations are shown in bold)¹.

Gene	SNP	Type	Trait	P-value	q-value	P-value*	q-value*	$\delta \pm SE$	A ₁	MAF
<i>PHKG1</i>	rs697732005 (3:16.830 Mb)	Splice region variant (G/A)	GM a*	0.88661	0.88661	0.68325	0.96577	-0.02 (0.142)	A	0.3443
<i>TGFBRAP1</i>	rs321173745 (3:49.516 Mb)	Missense variant (A/G)		0.00361	0.00902	0.03108	0.67220	0.549 (0.186)	G	0.1875
<i>SELENOI</i>	rs330820437 (3:112.635 Mb)	Missense variant (A/G)		0.00039	0.00196	0.01307	0.51778	0.643 (0.181)	G	0.1757
<i>HADHA</i>	rs81215086 (3:112.794 Mb)	Missense variant (G/A)		0.53993	0.67491	0.62966	0.96577	-0.102 (0.169)	A	0.2899
	rs344578723 (3:112.796 Mb)	Missense variant (G/A)		0.53466	0.67491	0.67980	0.96577	-0.104 (0.169)	A	0.2866
<i>COPA</i>	rs340853721 (4:90.163 Mb)	Splice region variant (T/C)	LD CE	0.90735	0.95684	0.79005	0.99942	0.014 (0.091)	T	0.4351
	rs333099339 (4:90.183 Mb)	Splice region variant (T/C)		0.87813	0.95684	0.88586	0.99942	0.017 (0.090)	T	0.4381
	rs80949931 (4:90.186 Mb)	Missense variant (A/G)		0.95684	0.95684	0.68990	0.99942	-0.002 (0.091)	A	0.4335
<i>PEA15</i>	rs329681990 (4:90.266 Mb)	Splice region variant (G/A)		0.85666	0.95684	0.58021	0.99942	-0.014 (0.091)	G	0.433
<i>CASQ1</i>	rs334946278 (4:90.280 Mb)	Splice region variant (G/A)		0.95267	0.95684	0.92240	0.99942	0.005 (0.104)	A	0.1304
<i>ATP1A2</i>	rs344748241 (4:90.356 Mb)	Splice region variant (G/A)		6.515E-06	7.167E-05	0.00006	0.02518	-0.325 (0.066)	G	0.497
<i>ATP8B2</i>	rs81382410			0.00285	0.01565	0.00256	0.21113		T	0.3345

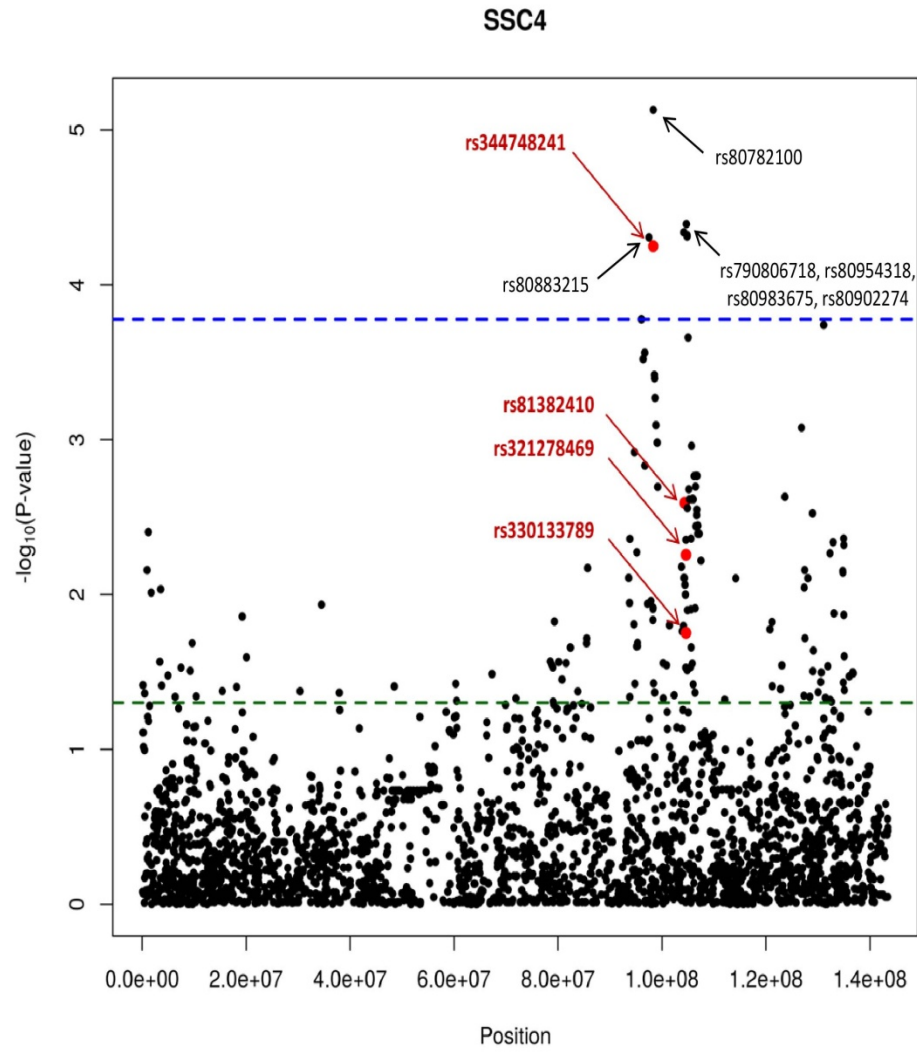
	(4:95.435 Mb)	Splice region variant (T/C)						-0.233 (0.077)		
CREB3L4	rs329686514 (4:95.717 Mb)	Missense variant (C/T)		0.08043	0.17695	0.22592	0.97957	-0.155 (0.088)	T	0.3063
	rs321278469 (4:95.717 Mb)	Missense variant (C/A)		0.00639	0.01757	0.00554	0.30475	-0.228 (0.083)	C	0.3084
	rs330133789 (4:95.721 Mb)	Missense variant (G/A)		0.00493	0.01757	0.01769	0.57188	0.254 (0.075)	A	0.3373
<i>CRTC2</i>	rs330198768 (4:95.740 Mb)	Intron variant (C/T)		0.32931	0.60373	0.56310	0.99942	-0.083 (0.085)	T	0.3687
<i>ACADSB</i>	rs81449951 (14:132.588 Mb)	Missense variant (C/A)	LD (C18:1) n-7	0.04036	0.08073	0.0424837	0.8322423	0.093 (0.045)	A	0.2109
GPR26	rs343087568 (14:133.182 Mb)	Splice region variant (A/G)		0.00333	0.01334	0.1269422	0.9956111	-0.096 (0.032)	G	0.4632
<i>CTBP2</i>	rs339956077 (14:134.334 Mb)	Splice region variant (G/A)		0.88166	0.88166	0.1269422	0.9956111	0.007 (0.046)	A	0.2094

328 ¹ The *P*-value and the *q*-value terms define the statistical significance of the association analysis before and after correcting for
329 multiple testing with a false discovery rate approach, respectively. The correction for multiple testing took into account the number of
330 candidate SNPs (2nd column of Table 1) mapping to each one of the SSC3 GM a* (5 SNPs), SSC4 CE (11 SNPs) and SSC14 LD
331 (C18:1) n-7 (3 SNPs) QTL. The *P*-value* and the *q*-value* terms define the statistical significance of the chromosome-wide
332 association analysis before and after correcting for multiple testing with a false discovery rate approach, respectively. In this case, the
333 correction for multiple testing took into account the number of markers in the Porcine SNP60 BeadChip mapping to pig chromosomes
334 SSC3 (3,123 SNPs), SSC4 (3,899 SNPs) and SSC14 (4,203 SNPs). Other terms that need to be defined are: δ , estimated allele

335 substitution effect and its standard error (SE); A₁, minor allele; MAF, minor allele frequency; GM a*, Minolta a* value (redness) in the
336 *gluteus medius* muscle; LD CE, electric conductivity in the *longissimus dorsi* muscle; and LD (C18:1) n-7, vaccenic acid content in the
337 *longissimus dorsi* muscle.

LEGENDS TO FIGURES

Figure 1: Manhattan plot depicting associations between electrical conductivity in the *longissimus dorsi* muscle and the genotypes of markers in the *ATPIA2* (rs344748241), *ATP8B2* (rs81382410) and *CREB3L4* (rs321278469 and rs330133789) loci plus 3,899 additional SNPs mapping to pig chromosome 4 (SSC4). The positions of these three genes are SSC4: 90.292-90.371 Mb (*ATPIA2*), SSC4: 95.426-95.446 Mb (*ATP8B2*) and SSC4: 95.714-95.723 Mb (*CREB3L4*). The green line represents the nominal *P-value* of significance, while the blue line indicates the *P-value* of significance after correcting for multiple testing with a false discovery rate approach (*q-value*). The rs344748241 SNP in the *ATPIA2* gene is located 23 kb away from the peak of the LD CE QTL, *i.e.* ALGA0026686 (rs80782100; 4:90.378 Mb) SNP, as reported by González-Prendes *et al.* (2017).



SUPPLEMENTARY DATA

Supplementary Table 1: Additional information about selected SNP and their potential impact and deleteriousness (SIFT).

Supplementary Figure 1: Graph depicting the magnitude of linkage disequilibrium among SNPs that showed significant associations with *longissimus dorsi* electric conductivity after correction for multiple testing at the chromosome-wide level. Here, the amount of linkage disequilibrium is expressed as r^2 as defined by Will & Robertson (1968) and such parameter was calculated with the *LD* function of *gaston* R package.

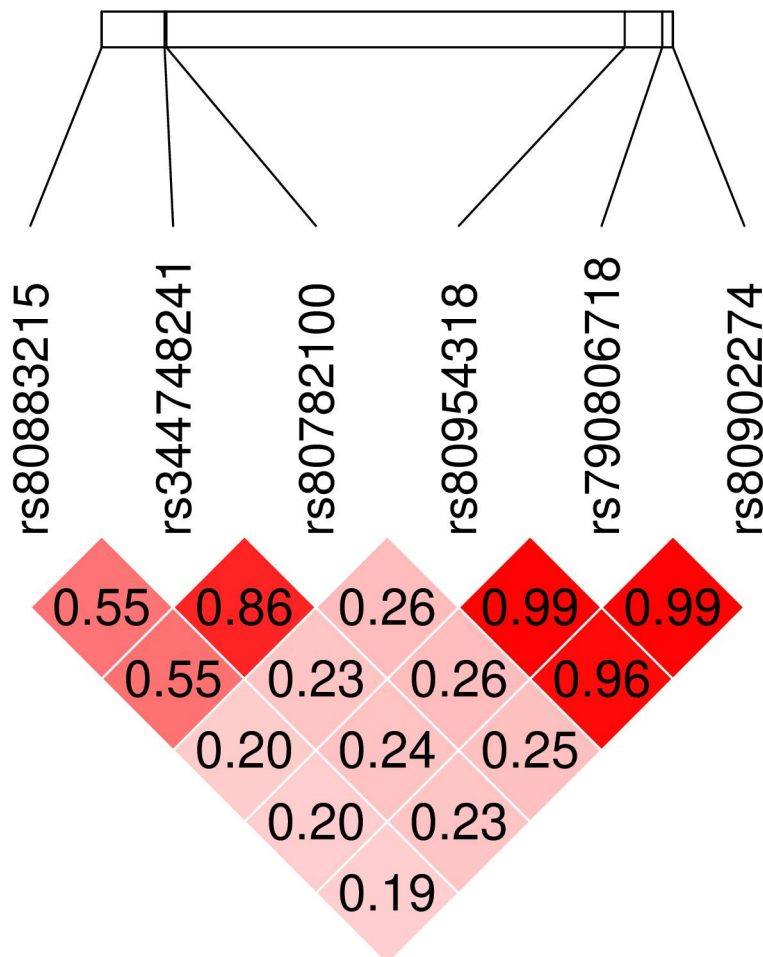
SUPPLEMENTARY DATA

Supplementary Table 1: Additional information about the set of selected SNP and their potential impact and deleteriousness (SIFT-based prediction).

SNP ID	Allele	Consequence	Impact	Symbol	SIFT
rs697732005	A	splice region variant,intron variant	LOW	<i>PHKG1</i>	-
rs321173745	G	missense variant	MODERATE	<i>TGFBRAP1</i>	tolerated(0.22)
rs330820437	G	missense variant	MODERATE	<i>SELENOI</i>	tolerated(1)
rs81215086	A	missense variant	MODERATE	<i>HADHA</i>	deleterious(0.04)
rs344578723	A	missense variant	MODERATE	<i>HADHA</i>	tolerated(0.81)
rs340853721	C	splice region variant,intron variant	LOW	<i>COPA</i>	-
rs333099339	C	splice region variant,intron variant	LOW	<i>COPA</i>	-
rs80949931	G	missense variant	MODERATE	<i>COPA</i>	tolerated(0.15)
rs329681990	A	splice region variant,intron variant	LOW	<i>PEA15</i>	-
rs334946278	A	splice region variant,synonymous variant	LOW	<i>CASQ1</i>	-
rs344748241	A	splice region variant,synonymous variant	LOW	<i>ATP1A2</i>	-
rs81382410	G	splice region variant,intron variant	LOW	<i>ATP8B2</i>	-
rs329686514	T	missense variant	MODERATE	<i>CREB3L4</i>	tolerated low confidence(0.05)
rs321278469	A	missense variant	MODERATE	<i>CREB3L4</i>	tolerated(0.24)
rs330133789	A	missense variant	MODERATE	<i>CREB3L4</i>	tolerated(0.32)
rs330198768	T	intron variant	MODIFIER	<i>CRTC2</i>	-
rs81449951	A	missense variant	MODERATE	<i>ACADSB</i>	tolerated(0.32)
rs343087568	G	splice region variant,intron variant	LOW	<i>GPR26</i>	-
rs339956077	T	splice region variant,intron variant	LOW	<i>CTBP2</i>	-

1 **Supplementary Figure 1:** Graph depicting the magnitude of linkage disequilibrium among
 2 SNPs that showed significant associations with *longissimus dorsi* electric conductivity after
 3 correction for multiple testing at the chromosome-wide level. Here, the amount of linkage
 4 disequilibrium is expressed as r^2 as defined by Hill & Robertson (1968) and such parameter
 5 was calculated with the *LD* function of the *gaston* R package.

6



7